Thai Journal of Mathematics
Special Issue (Annual Meeting in Mathematics, 2006) : 83–100

Sea Surface Elevation of the Primitive Equation Oceanic Model for the Gulf of Thailand

W. Wannawong, U. Humphries and A. Luadsong

Abstract : A sea surface elevation of the primitive equation oceanic model is proposed by studying in the Gulf of Thailand (GoT) from 98.54^oE to 105.54^oE in longitude and from 5.54^oN to 14.54^oN in latitude. The sea surface elevation is the displacement of the oceanic surface of waves which affects to the energy of the waves. In this paper, we study the sea surface elevation of motion of sea water which consists of wave interaction terms. They were derived via the sigma coordinate system by using the Princeton Oceanic Model (POM2k Version 2004) with topography from DBDB5 data and initial data of temperature and salinity from LEVITUS94 data.

Keywords : Primitive equation, Sea Surface Elevation, Sigma coordinate, Adiabatic process

1 Introduction

The sea surface elevation is the displacement of the ocean surface of waves which consists of the crest and trough. In this research, we study the Gulf of Thailand which is the important natural resource in Thailand. It has many uses for Thai people such as the marine fishery, crude oil processing to provide useful products, and places to go on holiday; Pattaya, Koh Chang, Koh Samet, and Koh Samui. The model of this study is the primitive equation model (Governing Equation) which is the partial differential equation (PDE). It is the non-linear equation which is very complicated and due to it being hard to solve the problem by an analytical method, we solve the problem by using the numerical method and discretizate to grid as Arakawa C-grid and also using the POM2k model [5] to find the answer of unknown variables of a non-linear system. In this research, we study the maximum of sea surface elevation and the area of the study covers from $98.54°E$ to $105.54°E$ in longitude and from $5.54°N$ to $14.54°N$ in latitude, which is shown in Figure 1. The POM2k model can predict the changing of the sea surface elevation for each week by using the initial data in March, July and November. In addition, it can specify the maximum of sea surface elevation in the GoT. The advantages of the

sea surface elevation are to save the human lives of those who live on the beach and to protect the important tourist places, as well as fishermen and oil rigs in the GoT for the whole year.

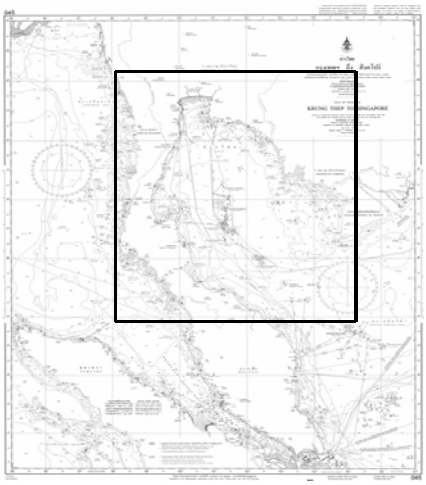

Figure 1: The boundary specific of the Gulf covers from $98.54°E$ to $105.54°E$ in longitude and from $5.54°N$ to $14.54°N$ in latitude (The Hydrologic Department, Royal Thai Navy).

2 The Model Equation

The mathematical modeling of this research is based on the primitive equation, which concerns with the basic equation as the equation of motion, the equation of continuity, and the hydrostatic equation. The spherical coordinates are the easiest to illustrate the principles of the equation, an advantage in using vector notation. Let (u, v, w) be the fluid velocities in the zonal, meridional and locally vertical direction respectively.

The horizontal equations of motion are

$$\frac{du}{dt} - A_m(\Delta u + \frac{1-\tan^2\theta}{a^2}u + \frac{2\tan\theta}{a^2\cos\theta}\frac{\partial v}{\partial\lambda}) + fv = -\frac{1}{\rho_0 a\cos\theta}\frac{\partial p}{\partial\lambda} + \frac{\partial}{\partial z}(A_{mv}\frac{\partial u}{\partial z}), \quad (1)$$

$$\frac{dv}{dt} - A_m(\Delta v + \frac{1-\tan^2\theta}{a^2}v + \frac{2\tan\theta}{a^2\cos\theta}\frac{\partial u}{\partial\lambda}) - fu = -\frac{1}{\rho_0 a}\frac{\partial p}{\partial\theta} + \frac{\partial}{\partial z}(A_{mv}\frac{\partial v}{\partial z}), \quad (2)$$

and

$$\frac{d}{dt} \equiv \frac{\partial}{\partial t} + v\frac{\partial}{a\partial\theta} + u\frac{\partial}{a\cos\theta\partial\lambda} + w\frac{\partial}{\partial z},$$

where A_m is the vertical eddy viscosity and A_{mv} is the vertical eddy viscosity, and the parameter $f = 2\Omega\sin\theta$ is the Coriolis parameter where Ω is the speed of

angular rotation of the Earth by $\Omega = 7.2921 \times 10^{-5}\ rad \cdot s^{-1}$.

The hydrostatic equation:

$$\frac{\partial p}{\partial z} = -\rho g, \tag{3}$$

where p is the local pressure.

The continuity equation:

$$\frac{\partial w}{\partial z} = -\frac{1}{a\cos\theta}\left(\frac{\partial v\cos\theta}{\partial\theta} + \frac{\partial u}{\partial\lambda}\right), \tag{4}$$

The temperature equation:

$$\frac{dT}{dt} = \frac{\partial}{\partial z}\left(A_{hv}\frac{\partial T}{\partial z}\right) + A_H\Delta T, \tag{5}$$

where T is the potential temperature.

The salinity equation:

$$\frac{dS}{dt} = \frac{\partial}{\partial z}\left(A_{hv}\frac{\partial S}{\partial z}\right) + A_H\Delta S, \tag{6}$$

where S is the potential salinity, A_{hv} is the vertical mixing coefficient and A_H is the horizontal mixing coefficient and the Laplacian operator is:

$$\Delta \equiv \frac{1}{a^2\cos\theta}\left[\frac{\partial}{\partial\theta}\left(\cos\theta\frac{\partial}{\partial\theta}\right) + \frac{1}{\cos\theta}\frac{\partial^2}{\partial\lambda^2}\right].$$

The state equation of sea water:

$$\rho = \rho(T, S, z), \tag{7}$$

where ρ is density.

Details of the primitive equations and the method of solution have been given by Cox (1984) [2]. Finally, the equations are solved for u, v, w, T, S, ρ and p variables by using the leap-frog finite difference technique to explain the circulation in the oceanic model (POM2k) for GoT.

3 The Numerical Method

From the POM2k, we use the assumption of fluid which is incompressible with the approximation methods to drive the model (i.e. Thin-shell, Hydrostatic and Boussinesq approximations).

3.1 The Perturbed Thermodynamic Variables

There are four thermodynamic variables, i.e. p, ρ, T and S, in equations (1)-(7). In order to minimize computational errors, the perturbed variables can be defined

as:

$$\acute{p} \equiv p - \tilde{p}(\lambda, \theta, z), \qquad \acute{\rho} \equiv \rho - \tilde{\rho}(\lambda, \theta, z),$$
$$\acute{T} \equiv T - \tilde{T}(\lambda, \theta, z), \qquad \acute{S} \equiv S - \tilde{S}(\lambda, \theta, z),$$

where $\tilde{p}(\lambda, \theta, z)$, $\tilde{\rho}(\lambda, \theta, z)$, $\tilde{T}(\lambda, \theta, z)$ and $\tilde{S}(\lambda, \theta, z)$ are the standard distributions of pressure, density, temperature and salinity respectively. $\tilde{T}(\lambda, \theta, z)$ and $\tilde{S}(\lambda, \theta, z)$ can be determined by using observed data, and then according to

$$\begin{aligned} \frac{\partial \tilde{p}(\lambda, \theta, z)}{\partial z} &= -\tilde{\rho}(\lambda, \theta, z) g, \\ \tilde{p}(\lambda, \theta, 0) &= \tilde{p}_{as}(\lambda, \theta). \end{aligned}$$

We derive the mean density by $\tilde{\rho}(\lambda, \theta, z) \equiv \rho(\tilde{T}, \tilde{S}, z)$ and pressure by $\tilde{p}(\lambda, \theta, z) = \tilde{p}_{as}(\lambda, \theta) + g\int_z^0 \tilde{\rho}(\lambda, \theta, t)dt$, where $\tilde{p}_{as}(\lambda, \theta)$ is the sea level air pressure computed, based on the atmospheric data.

3.2 Sigma Coordinate

The sigma coordinate (pressure coordinate) is a function of density where the density is a function of temperature and salinity. In order to separate water in the GoT in several layers, the vertical sigma coordinate is used. In the sigma coordinate system, the primitive equations from z-coordinate (λ, θ, z, t) are transformed to the vertical sigma coordinate $(\lambda^*, \theta^*, \sigma, t^*)$ with the relationships:

$$\lambda^* = \lambda, \quad \theta^* = \theta, \quad \sigma = \frac{z - \eta}{H + \eta} \quad \text{and} \quad t^* = t$$

where $H(\lambda, \theta)$ is the bottom topography and η is the sea surface elevation. σ ranges from $\sigma = 0$ at $z = \eta$ to $\sigma = -1$ at $z = -H(\lambda, \theta)$.

3.3 Mode Splitting

It is desirable in terms of computer economy to separate out vertically integrated equations (external mode) from the vertical structure equations (internal mode). The horizontal currents are defined as:

$$u = \bar{u} + \acute{u}, \qquad v = \bar{v} + \acute{v}.$$

where $(\bar{u}, \bar{v})$ are the vertically integrated mass flux:

$$\bar{u} = \int_{-1}^{0} u d\sigma, \qquad \bar{v} = \int_{-1}^{0} v d\sigma$$

and $(\acute{u}, \acute{v})$ are in the baroclinic mode, and have no depth average.

3.4 Finite Difference Techniques

We use the perturbed thermodynamic variables, sigma coordinate and the staggered C-grid, which are shown in Figure 2, where Ψ are Temperature (T) and Salinity (S), Sea Surface Elevation (η), and Bottom topography (H), etc [1].

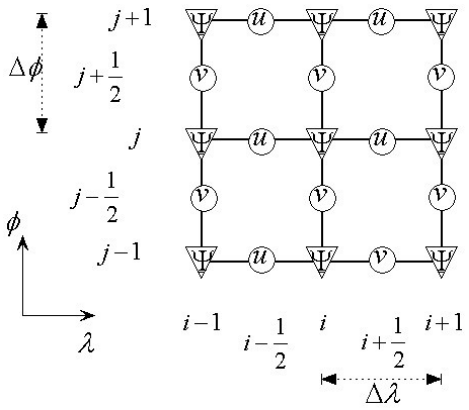

Figure 2: The staggered C-grid of variables in horizontal coordinates.

The k^{th} box has thickness $\Delta\sigma_k$. The horizontal grid is C-grid. The relative positions of the variables on the staggered grid are shown in Figure 3, where $k = 1, 2,...,k_\circ$ and $k_\circ$ is the total number of vertical layers.

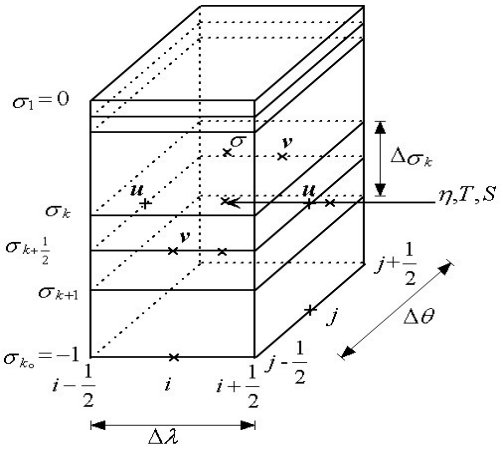

Figure 3: The locations of the variables on the finite difference grid.

The finite difference operators and averaging operators are defined as:

$$\begin{aligned}(\frac{\partial G}{\partial \lambda})_i &\approx \frac{G_{i+\frac{1}{2}}-G_{i-\frac{1}{2}}}{\Delta\lambda} \equiv \frac{1}{\Delta\lambda}(\delta_\lambda G)_i,\\ G_i &\approx \frac{G_{i+\frac{1}{2}}+G_{i-\frac{1}{2}}}{2} \equiv (\bar{G}^\lambda)_i,\end{aligned}$$

where G is the discrete variable. The operators with respect to latitude θ, vertical coordinate σ and time t are similar to those above. By using these discrete operators, the spatial finite difference to barotropic (vertically integrated) equations can be written as:

$$\begin{aligned}\Big(\frac{\partial \bar{u}}{\partial t}\Big)_{i+\frac{1}{2},j} &= \Big(\frac{1}{\rho_0 a\cos\theta}\frac{\delta_\lambda \acute{p}_{as}}{\Delta\lambda}\Big)_{i+\frac{1}{2},j} - (f\bar{\bar{v}}^{\lambda\theta})_{i+\frac{1}{2},j} + (\overline{\acute{p}_\lambda})_{i+\frac{1}{2},j} + \Big\{\Big(\overline{\overline{\acute{g}\sigma}}^{\lambda} - \frac{g\overline{\overline{\tilde{\rho}\sigma}}^{\lambda}}{\rho_\circ}\Big)\frac{\delta_\lambda H}{a\cos\theta\Delta\lambda}\Big\}_{i+\frac{1}{2},j}\\ &\quad +(\overline{\tilde{p}_\lambda})_{i+\frac{1}{2},j} + \Big\{(\overline{\overline{\acute{g}\sigma}}^{\lambda} + \bar{\bar{\acute{g}}}^{\lambda} - \tfrac{g}{\rho_\circ}(\overline{\overline{\tilde{\rho}\sigma}}^{\lambda} + \bar{\bar{\tilde{\rho}}}^{\lambda} + \rho_\circ))\tfrac{\delta_\lambda \eta}{a\cos\theta\Delta\lambda}\Big\}_{i+\frac{1}{2},j} + (\overline{LB})_{i+\frac{1}{2},j}, \qquad (8)\\ \Big(\frac{\partial \bar{v}}{\partial t}\Big)_{i,j+\frac{1}{2}} &= \Big(\frac{1}{\rho_0 a}\frac{\delta_\theta \acute{p}_{as}}{\Delta\theta}\Big)_{i,j+\frac{1}{2}} - (f\bar{\bar{u}}^{\lambda\theta})_{i,j+\frac{1}{2}} + (\overline{\acute{p}_\theta})_{i,j+\frac{1}{2}} + \Big\{\Big(\overline{\overline{\acute{g}\sigma}}^{\theta} - \frac{g\overline{\overline{\tilde{\rho}\sigma}}^{\theta}}{\rho_\circ}\Big)\frac{\delta_\theta H}{a\Delta\theta}\Big\}_{i,j+\frac{1}{2}}\\ &\quad +(\overline{\tilde{p}_\theta})_{i,j+\frac{1}{2}} + \Big\{(\overline{\overline{\acute{g}\sigma}}^{\theta} + \bar{\bar{\acute{g}}}^{\theta} - \tfrac{g}{\rho_\circ}(\overline{\overline{\tilde{\rho}\sigma}}^{\theta} + \bar{\bar{\tilde{\rho}}}^{\theta} + \rho_\circ))\tfrac{\delta_\theta \eta}{a\Delta\theta}\Big\}_{i,j+\frac{1}{2}} + (\overline{TB})_{i,j+\frac{1}{2}} \qquad (9)\\ \Big(\frac{\partial \eta}{\partial t}\Big)_{i,j} &= -\Big\{\frac{1}{a\cos\theta}\Big[\frac{\delta_\theta}{\Delta\theta}\overline{(H+\eta)}^{\theta}\bar{v}\cos\theta + \frac{\delta_\lambda}{\Delta\lambda}\overline{(H+\eta)}^{\lambda}\bar{v}\Big]\Big\}_{i,j} \qquad (10)\end{aligned}$$

The spatial finite difference of fully baroclinic equations are taken to be:

$$\begin{aligned}\Big(\frac{\partial u}{\partial t}\Big)_{i+\frac{1}{2},j,k+\frac{1}{2}} &= -\Big\{\frac{1}{a\cos\theta}\Big(\frac{\delta_\lambda \acute{p}}{\rho_0\Delta\lambda} + \frac{\delta_\lambda \tilde{p}}{\Delta\lambda}\Big)\Big\}_{i+\frac{1}{2},j,k+\frac{1}{2}} + \Big\{\bar{\acute{g}}^{\lambda}\frac{\delta_\lambda}{a\cos\theta\Delta\lambda}\Big[\sigma(H+\eta)+\eta\Big]\Big\}_{i+\frac{1}{2},j,k+\frac{1}{2}}\\ &\quad -\Big\{\frac{g\bar{\tilde{\rho}}^{\lambda}}{\rho_\circ}\frac{\delta_\lambda}{a\cos\theta\Delta\lambda}\Big[\sigma(H+\eta)+\eta\Big]\Big\}_{i+\frac{1}{2},j,k+\frac{1}{2}} - (f\bar{v}^{\lambda\theta})_{i+\frac{1}{2},j,k+\frac{1}{2}} + (LB)_{i+\frac{1}{2},j,k+\frac{1}{2}} \qquad (11)\\ \Big(\frac{\partial v}{\partial t}\Big)_{i,j+\frac{1}{2},k+\frac{1}{2}} &= -\Big\{\frac{1}{\rho_0 a}\Big(\frac{\delta_\theta \acute{p}}{\Delta\theta} + \frac{\delta_\theta \tilde{p}}{\Delta\theta}\Big)\Big\}_{i,j+\frac{1}{2},k+\frac{1}{2}} + \Big\{\bar{\acute{g}}^{\theta}\frac{\delta_\theta}{a\Delta\theta}\Big[\sigma(H+\eta)+\eta\Big]\Big\}_{i,j+\frac{1}{2},k+\frac{1}{2}}\\ &\quad -\Big\{\frac{g\bar{\tilde{\rho}}^{\lambda\theta}}{\rho_\circ}\frac{\delta_\theta}{a\Delta\theta}\Big[\sigma(H+\eta)+\eta\Big]\Big\}_{i,j+\frac{1}{2},k+\frac{1}{2}} + (f\bar{u}^{\theta\lambda})_{i,j+\frac{1}{2},k+\frac{1}{2}} + (TB)_{i,j+\frac{1}{2},k+\frac{1}{2}} \qquad (12)\\ (\acute{p})_{i,j,k+\frac{1}{2}} &= (\acute{p}_{as}+\rho_\circ g\eta)_{i,j,1} - \rho_\circ\Big\{\int_\sigma^0 (H+\eta)\acute{g}d\acute{\sigma}\Big\}_{i,j,k+\frac{1}{2}} \qquad (13)\end{aligned}$$

The spatial finite difference of temperature and salinity equations are:

$$
\begin{aligned}
(\acute{T})_{i,j,k+\frac{1}{2}} &= -\Big(\bar{v}^{\theta}\frac{\delta_\theta \overline{T}^{\theta}}{a\Delta\theta}\Big)_{i,j,k+\frac{1}{2}} + A_H\Big\{\frac{1}{a^2\cos\theta}\Big(\frac{\delta_\theta(\cos\theta\delta_\theta T)}{(\Delta\theta)^2}\Big) + \frac{1}{a^2\cos^2\theta}\Big(\frac{\delta_\lambda(\delta_\lambda T)}{(\Delta\lambda)^2}\Big)\Big\}_{i,j,k+\frac{1}{2}} \\
&\quad -\Big(\bar{\acute{\sigma}}^{\sigma}\frac{\delta_\sigma \overline{T}^{\sigma}}{\Delta\sigma}\Big)_{i,j,k+\frac{1}{2}} + \{(\frac{1}{H+\eta})^2\frac{\delta_\sigma}{\Delta\sigma}(A_{hv}\frac{\delta_\sigma T}{\Delta\sigma})\}_{i,j,k+\frac{1}{2}} - (\bar{u}^{\lambda}\frac{\delta_\lambda \overline{T}^{\lambda}}{a\cos\theta\Delta\lambda})_{i,j,k+\frac{1}{2}}
\end{aligned}
\tag{14}
$$

$$
\begin{aligned}
(\acute{S})_{i,j,k+\frac{1}{2}} &= -(\bar{v}^{\theta}\frac{\delta_\theta \overline{S}^{\theta}}{a\Delta\theta})_{i,j,k+\frac{1}{2}} + A_H\{\frac{1}{a^2\cos\theta}(\frac{\delta_\theta(\cos\theta\delta_\theta S)}{(\Delta\theta)^2}) + \frac{1}{a^2\cos^2\theta}(\frac{\delta_\lambda(\delta_\lambda S)}{(\Delta\lambda)^2})\}_{i,j,k+\frac{1}{2}} \\
&\quad -(\bar{\acute{\sigma}}^{\sigma}\frac{\delta_\sigma \overline{S}^{\sigma}}{\Delta\sigma})_{i,j,k+\frac{1}{2}} + \{(\frac{1}{H+\eta})^2\frac{\delta_\sigma}{\Delta\sigma}(A_{hv}\frac{\delta_\sigma S}{\Delta\sigma})\}_{i,j,k+\frac{1}{2}} - (\bar{u}^{\lambda}\frac{\delta_\lambda \overline{S}^{\lambda}}{a\cos\theta\Delta\lambda})_{i,j,k+\frac{1}{2}}
\end{aligned}
\tag{15}
$$

where:

$$
\begin{aligned}
\overline{\acute{g}\sigma} &= \int_{-1}^{0}\acute{g}\sigma d\sigma = \sum_{k=1}^{k_0}\acute{g}\sigma_k\Delta\sigma_k, \qquad \acute{g} = -\frac{\acute{\rho}}{\rho_0}g \quad \text{is buoyancy,} \\
\acute{p}_\lambda &= \frac{\partial}{a\cos\theta\partial\lambda}\int_{\sigma}^{0}(H+\eta)\acute{g}d\acute{\sigma}, \qquad \tilde{p}_\lambda = -\frac{1}{\rho_0 a\cos\theta}\frac{\partial\tilde{p}}{\partial\lambda}, \\
\acute{p}_\theta &= \frac{\partial}{a\partial\theta}\int_{\sigma}^{0}(H+\eta)\acute{g}d\acute{\sigma}, \qquad \tilde{p}_\theta = -\frac{1}{\rho_0 a}\frac{\partial\tilde{p}}{\partial\theta}, \\
LB &= -L(u) + \Big(\frac{1}{H+\eta}\Big)^2\frac{\partial}{\partial\sigma}\Big(A_{mv}\frac{\partial u}{\partial\sigma}\Big) + F_1^{\lambda} + F_2^{\lambda}, \\
TB &= -L(v) + \Big(\frac{1}{H+\eta}\Big)^2\frac{\partial}{\partial\sigma}\Big(A_{mv}\frac{\partial u}{\partial\sigma}\Big) + F_1^{\theta} + F_2^{\theta}, \\
L(F) &= v\frac{\partial F}{a\partial\theta} + u\frac{\partial F}{a\cos\theta\partial\lambda} + \acute{\sigma}\frac{\partial F}{\partial\sigma}, \qquad (F \equiv u, v, T \text{ or } S) \\
F_1^{\lambda} &= A_m\Big[\Delta u + \frac{1-\tan^2\theta}{a^2}u + \frac{2\tan\theta}{a^2\cos\theta}\frac{\partial v}{\partial\lambda}\Big], \\
F_2^{\lambda} &= A_m\Big[XX(u) - \frac{2\tan\theta}{a^2\cos\theta}\Big(\frac{1}{H+\eta}\Big)\frac{\partial}{\partial\lambda}\Big[\sigma(H+\eta)\Big]\frac{\partial v}{\partial\sigma}\Big], \\
F_1^{\theta} &= A_m\Big[\Delta v + \frac{1-\tan^2\theta}{a^2}v + \frac{2\tan\theta}{a^2\cos\theta}\frac{\partial u}{\partial\lambda}\Big], \\
F_2^{\theta} &= A_m\Big[XX(v) - \frac{2\tan\theta}{a^2\cos\theta}\Big(\frac{1}{H+\eta}\Big)\frac{\partial}{\partial\lambda}\Big[\sigma(H+\eta)\Big]\frac{\partial u}{\partial\sigma}\Big],
\end{aligned}
$$

$XX(F)$ is the term which is generated by the Laplacian operator from z-coordinate to σ-coordinate.

The primitive equations are in the partial differential equation form.

4 Computational Details

To start the model computation, current should be defined at the initial stage. The model starts computation assuming the water velocity is zero everywhere. The model requires initial conditions of temperature, salinity and bottom topography from observations at each grid point for running the model. We assume that within the condition of the adiabatic process about the closed system and the closed boundary and also neglect the problem about the motion of sea water, which is a cause of wind stress at the sea surface (the motion of the circulation is moved by the nature of oceanography) and neglect the friction force at the bottom topography. The model bathymetry is driven from DBDB5 dataset (U.S. Naval Oceanographic Office, 1983) [6] which provides ocean depths every $5^{'}$ of latitude and longitude directions which is shown in Figure 4 and the temperature [3] and salinity [4] fields are initialized from Levitus94 dataset (Levitus, 1994) which are shown in Figure 5 to Figure 7. The resolution of the LEVITUS94 data file is $1^{\circ}\times 1^{\circ}$ degree in longitude and latitude directions. From the numerical method, we solve the the system of equations by using the POM2k (version 2004) and consider only the sea surface elevation in the external mode. Therefore, we use the initial data at the sea surface.

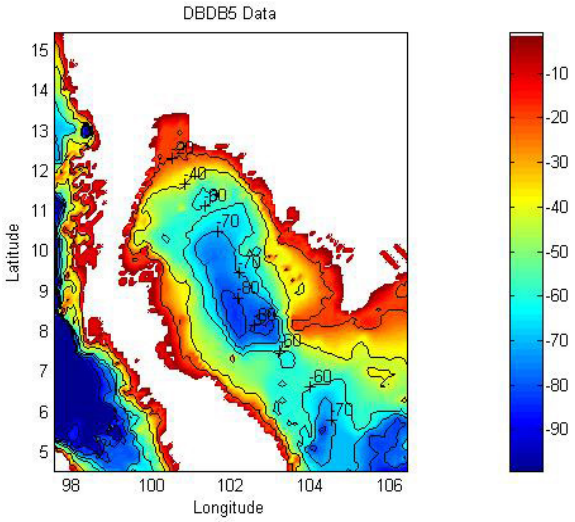

Figure 4: The Initial Data of Topography (m).

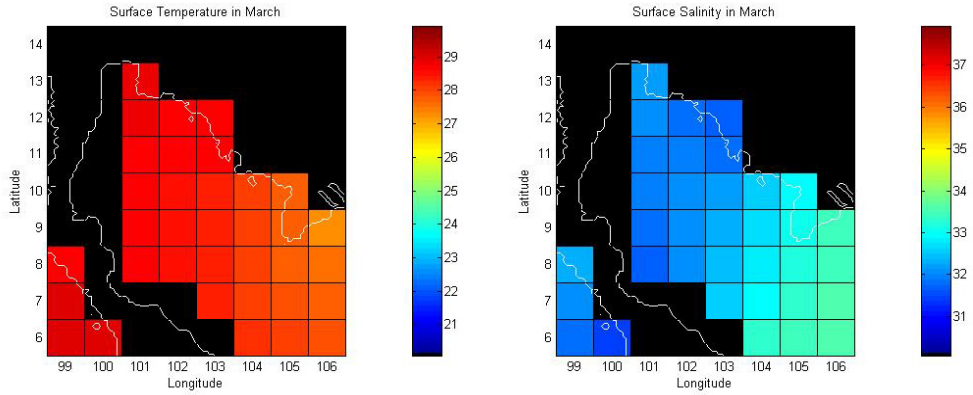

(a) (b)

Figure 5: The Initial Data of (a) Temperature (°C) and (b) Salinity (*ppt*) at the surface in March 1993.

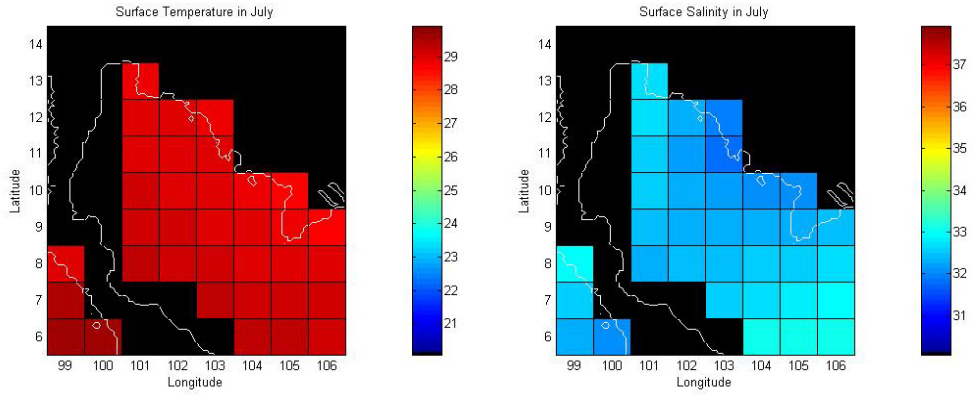

(a) (b)

Figure 6: The Initial Data of (a) Temperature (°C) and (b) Salinity (*ppt*) at the surface in July 1993.

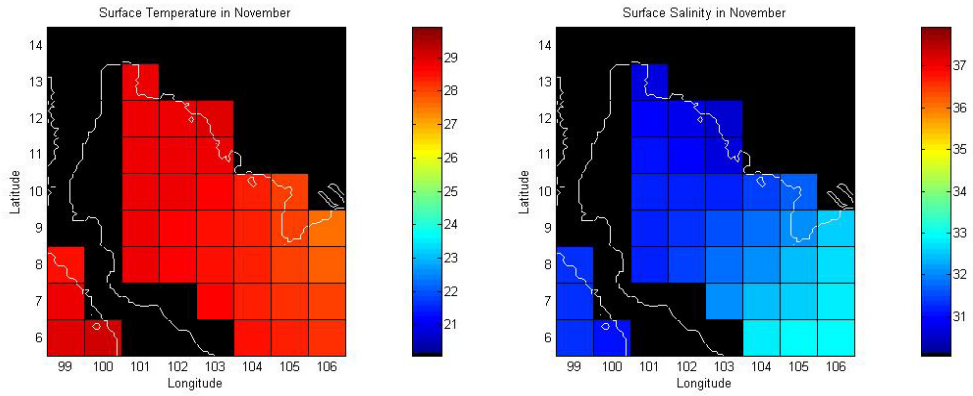

(a) (b)

Figure 7: The Initial Data of (a) Temperature (°C) and (b) Salinity (*ppt*) at the surface in November 1993.

It's collected in different resolutions and is not available at the model grid. In order to produce grided fields of data for using in the model, the interpolation methods are used. The data in the interior grid points are interpolated by bilinear interpolation and the boundary grid points interpolated by cubic spline interpolation and applied to the GoT. Figure 8 shows the topography and Figure 9 to Figure 11 show the temperature and salinity at the sea surface in March, July and November 1993 by using the interpolations.

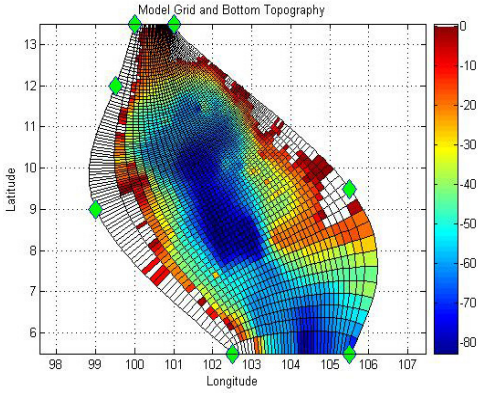

Figure 8: The Initial Data of Topography (m) by using the interpolation.

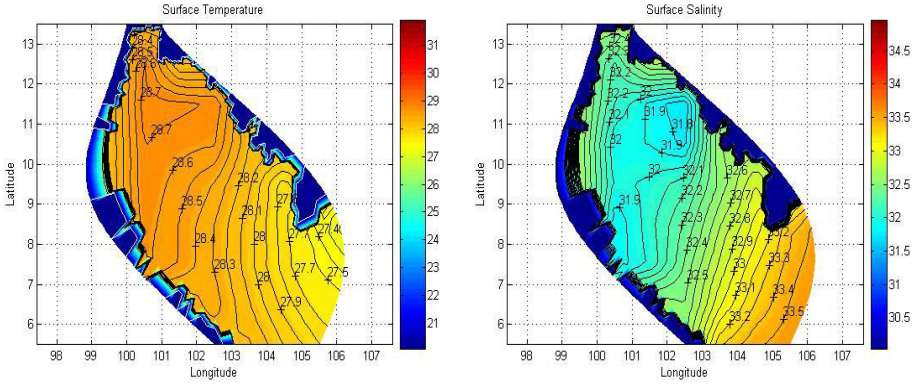

(a) (b)

Figure 9: The Initial Data of (a) Temperature (°C) and (b) Salinity (*ppt*) by using the interpolation in March.

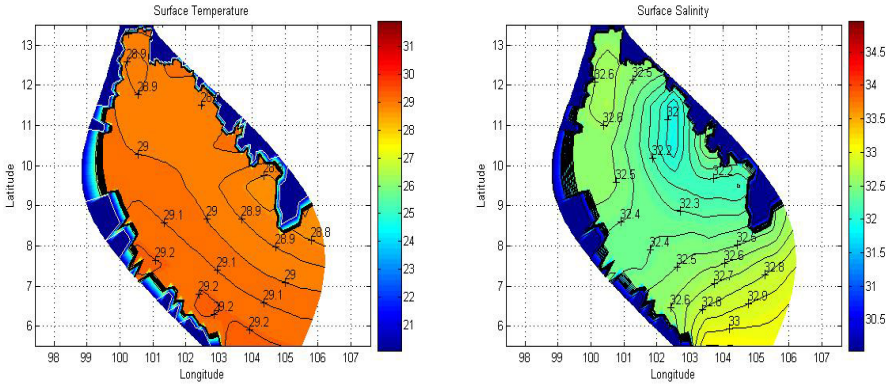

(a) (b)

Figure 10: The Initial Data of (a) Temperature (°C) and (b) Salinity (*ppt*) by using the interpolation in July.

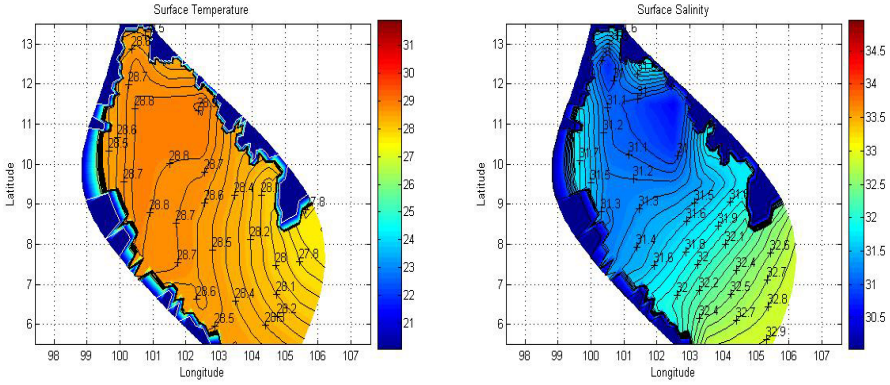

(a) (b)

Figure 11: The Initial Data of (a) Temperature (°C) and (b) Salinity (*ppt*) by using the interpolation in November.

The POM2k model has been set up with 37×97 grid points in the horizontal and 10 sigma vertical levels for the GoT. Since the GoT connects to the South China Sea, so we can use the South China Sea as a open boundary for the GoT. The rectangular grid is shown in Figure 12(a). It is taken for the domain of the model. In this research, the GoT is the curvilinear grid and is shown in Figure 12(b). Each of the curvilinear grid angles is almost 90° thus we can consider that it seems like the rectangular grid, which is shown in Figure 13(a). The west ($99.0°E$) and east ($105.54°E$) boundaries are places through U-points, whereas south ($5.54°N$) and the north ($13.54°N$) boundaries are through V-points. Let the west, east, north and south boundaries of the model be a rigid wall, i.e. $u_{\frac{1}{2},j}$=0, $v_{I-\frac{1}{2},j}$=0, $v_{i,\frac{1}{2}}$=0 and $v_{i,J-\frac{1}{2}}$=0 are shown in Figure 13(b).

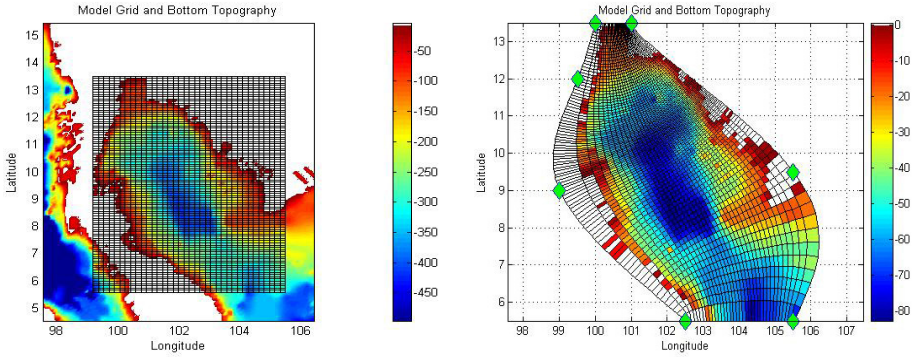

(a) (b)

Figure 12: (a) The rectangular grid and (b) the curvilinear grid are the closed boundary specific of the Gulf covers from $99.0°E$ to $105.54°E$ in longitude and from $5.54°N$ to $13.54°N$ in latitude.

Finally for our model, the program had the following steps: generated the horizontal and vertical grid; read bottom topography and interpolate to the grid; read temperature and salinity and interpolate to the grid; wrote grid and initial conditions for model; wrote the initial data and use it to drive the POM2k; and, last of all, wrote the results for the Matlab plot. In calculating, the horizontal grid sizes of the model are chosen to be $\Delta\lambda \leq 55\ km$ and $\Delta\phi \leq 45\ km$. The time step sizes are chosen as $\Delta t_i = 900\ s$ in the internal mode, $\Delta t_e = 30\ s$ in the external mode and α= 0.2250 (weak filter) for the development and stability process.

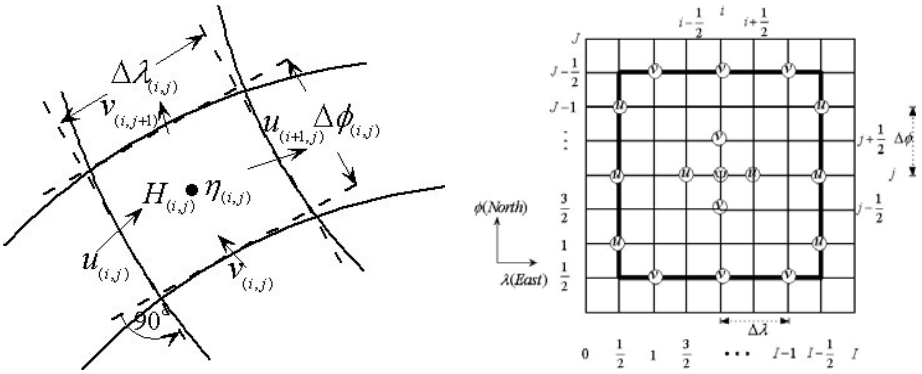

(a) (b)

Figure 13: (a) The curvilinear grid and (b) the rectangular grid with staggered C-grid, where the west, east, north and south boundaries are a rigid wall.

5 Results and Discussion

The initial data of bottom topography, temperature and salinity after driving the model for 53 weeks (one year) can classify for three seasons such as Summer, Rainy season and Winter. There are three months that are the example of each seasons: March in Summer; July in Rainy season and November in Winter. After input of the initial data of the bottom topography, temperature and salinity by using the interpolation of the monthly mean, the POM2k model is driven for a week in each of those months (i.e. March, July and November) so that we can consider the affect of the depth of topography, temperature and salinity to the sea surface elevation in those months of each of those seasons. The results after driving the model at the 1^{st} and 53^{rd} weeks are shown in Figure 14 and Figure 15 respectively.

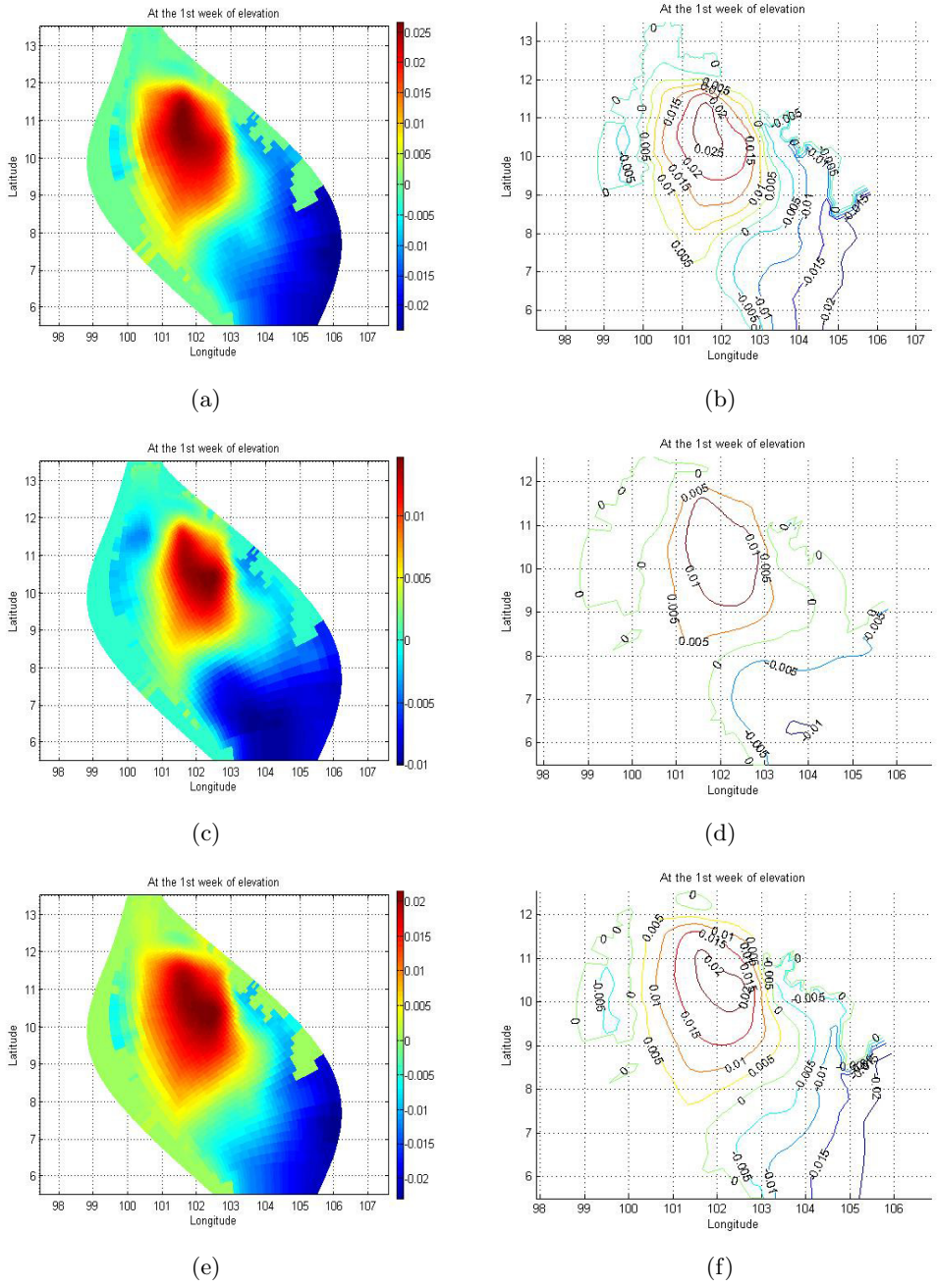

Figure 14: Sea Surface Elevation; Contour lines of Sea Surface Elevation after driving the model at the 1^{st} week in (a),(b) March; (c),(d) July; and (e),(f) November.

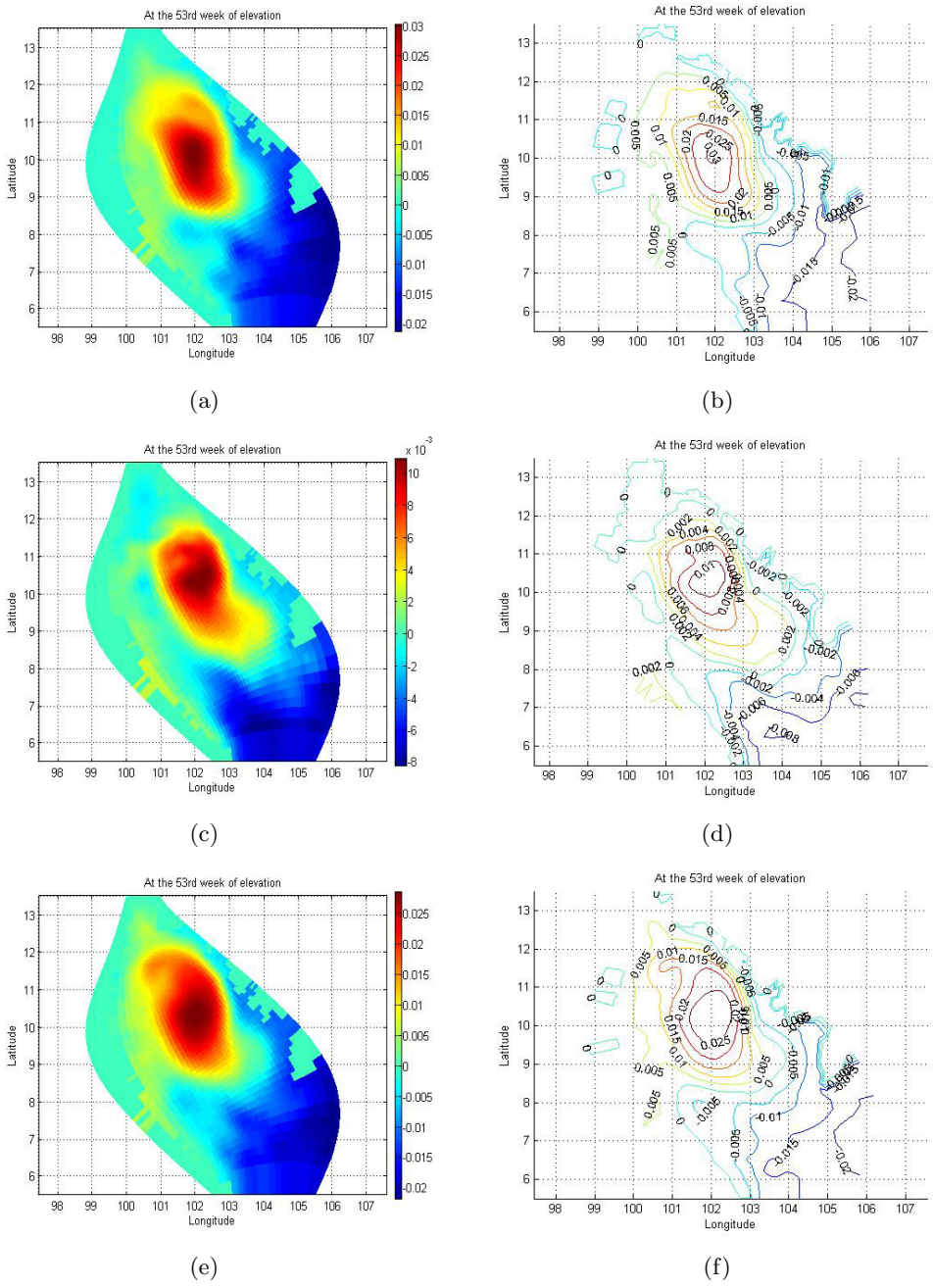

Figure 15: Sea Surface Elevation; Contour lines of Sea Surface Elevation after driving the model at the 53^{rd} week in (a),(b) March; (c),(d) July; and (e),(f) November.

After driving the model, we find that the maximum amplitude of the sea surface elevation is in the upper part of the GoT, which is the basin area. The sea surface elevation in the positive is called the crest and the sea surface elevation in the negative is called the trough. The connection between the crest and the trough is balance, which affects to the sea surface elevation and goes to zero. The sea surface elevations in the upper part of the GoT are positive, in the lower part of the GoT are negative and in the middle part of the GoT, including the land, are zero. From the calculation by using the POM2k model, the results of contour lines in March, July and November are shown in Figure 14(b), 14(d), 14(f), 15(b), 15(d) and 15(f) respectively. The maximum amplitude of the sea surface elevation at the 1^{st} week is different from the 53^{rd} week, which is shown in Table 1.

Run time days	Maximum of Sea Surface Elevation (m)		
	Mar	Jul	Nov
1. At the 1^{st} week	0.02689	0.01481	0.02171
2. At the 53^{rd} week	0.03056	0.01103	0.02889

From Table 1, in March, we find that the maximum amplitude of the sea surface elevation at the 53^{rd} week is higher than the 1^{st} week, thus the height of wave at the 53^{rd} week is higher than at the 1^{st} week. Otherwise, in July, the maximum of the sea surface elevation at the 53^{rd} week is less than at the 1^{st} week, and that make the heights of waves at the 53^{rd} week less than another one. Finally, in November, the maximum amplitude of the sea surface elevation at the 53^{rd} week is higher than at the 1^{st} week, thus the height of wave at the 53^{rd} week is higher than at the 1^{st} week. Many factors (i.e. pressure field and wind field) affect to the sea surface elevation. In this research, we concentrate on the behavior of the sea surface elevation from the topography with the initial data of temperature and salinity. From the POM2k Model, we find that the motion of sea water flows from the lower part of the GoT through the deep water channel and finally to the upper part of the GoT. Furthermore, the advantage of the model is that it can predict the sea surface elevation for many years later.

6 Conclusions

The model can indicate the meteorological situation from rapid change of the depth mean current and sea surface elevation. According to Zeng et al. [7]. It has been shown that the major characteristics of the model are as follows:

1. The model is defined by a typical non-negative operator equation, so the computational stability is guaranteed.

2. The staggered C-grid is adopted for saving computer storage and time. The C-grid is also conveniently applied to the problem with irregular boundary.

3. According to the properties of the physical process, the schemes can be split into three systems, which are solved one by one for saving computer time.

4. The structure of the scheme is very simple. It conserves the energy properties of original partial differential equations and is very convenient for writing a computational program.

For the validation of the model results very limited observations on sea level were available during the period of sea surface elevation. It may be seen from the plots in Figure 14 to Figure 15 (POM2k Model) that computed sea surface elevations are in fairly good agreement at the time of landfall with available time series observations at three coastal stations close to landfall. However, high sea surface elevation after the landfall, as seen in observations, could not be produced by the model.

7 Acknowledgements

The author would like to thank the computer laboratory of the mathematics department, faculty of science, King Mongkut's University of Technology Thonburi for advanced research and I would like to express my sincere appreciation to Asst. Prof. Usa Wannasingha Humphries, my supervisor, for giving her time to me generously, always patiently explaining new and difficult concepts, and always being encouraging during the past year. I would also like to thank Anirut Luadsong for his idea about the interpolation methods with me anytime during the past year. In addition, I would like to thank Nitima Aschariyaphotha and Prasertsak Ekphisutsuntorn for the observations about the datasets, subroutine results and for giving me insights on how the test cases should work; they helped me to find a bug in the POM2k version 2004 model, and made many comments on various drafts of the research. Finally, I would like to thank Asst. Prof. Marasri Nawjumpa and the mathematics department, faculty of science, Ubon Ratchathani Rajabhat University for advanced research and my family for putting up with the stress of preparing for the conference, and especially, Mr. Jonathan David Humphries and Chittamas Suksawaeng for encouragement and comments on the English skill of this research and to try again. Thanks.

References

[1] Arakawa, A., and V. R. Lamb, Computational Design of the Basic Dynamical Processes of the UCLA General Circulation Model, *Methods in Computational Physics*, edited by Chang J., Academic, San Diego, Calif., **17**, 173–265, 1977.

[2] Cox, M. D., A primitive equation, three-dimensional model of the ocean, *Tech. Rep. 1*, Ocean Group, Geophys. Fluid Dyn. Lab., NOAA, Princeton, N.J., 1984.

[3] Levitus, S. and Boyer, T., World Ocean Atlas 1994, Temperature, NOAA Atlas NESDIS, **4**, 117pp., 1994a.

[4] Levitus, S., Burgett, R. and Boyer, T., World Ocean Atlas 1994, Salinity, NOAA Atlas NESDIS, **3**, 99pp., 1994b.

[5] Mellor, G. L., Users Guide for a Three-Dimensional, Primitive Equation, *Numerical Ocean Model*, Princeton University, 2004.

[6] U.S. Naval Oceanographic Office and the U.S. Naval Ocean Research and Development Activity, DBDB5 (Digital Bathymetric Data Base-5 Minute Grid), U.S.N.O.O., Bay St. Louis, 1983.

[7] Zeng, Q., Ji, Z. and Li, R., The Construction of Difference Schemes for Evolution Equations and the Numerical Simulation of offshore Currents, *Chinese Journal of Atmospheric Sciences*, (Special issue for the 60^{th} anniversary of the foundation of IAP), 166–175, 1988.

(Received 25 May 2006)

W. Wannawong
Department of Mathematics
Faculty of Science
Ubon Ratchathani Rajabhat University
Ubon Ratchathani 34000, THAILAND.
e-mail: `worachataj@yahoo.com`

U. Humphries and A. Luadsong
Department of Mathematics
Faculty of Science
King Mongkut's University of Technology Thonburi
Bangkok 10140, THAILAND.